


Article

The Scale Model Room Approach to Test the Performance of Airtight Membranes to Control Indoor Radon Levels and Radiation Exposure

Manuela Portaro ¹, Iliara Rocchetti ¹, Paola Tuccimei ^{1,*}, Gianfranco Galli ² , Michele Soligo ¹, Cristina Longoni ³ and Dino Vasquez ³

¹ Dipartimento di Scienze, Università degli Studi “Roma Tre”, Largo San Leonardo Murialdo 1, 00146 Rome, Italy; manuela.portaro@uniroma3.it (M.P.); ilia.rocchetti@uniroma3.it (I.R.); michele.soligo@uniroma3.it (M.S.)

² Istituto Nazionale di Geofisica e Vulcanologia, Sezione Roma 1, Via Vigna Murata 605, 00143 Rome, Italy; gianfranco.galli@ingv.it

³ Mapei S.p.A., Waterproofing Line, Via Carlo Cafiero 22, 20158 Milano, Italy; c.longoni@mapei.it (C.L.); d.vasquez@mapei.it (D.V.)

* Correspondence: paola.tuccimei@uniroma3.it

Abstract: Indoor radon is one of the most significant contributors to lung cancer after smoking. Mitigation strategies based on protecting buildings with radon barrier materials, combined with home ventilation or room pressurization, are regularly used. A scale model room made from a porous ignimbrite rich in radon precursors was used as an analogue to test the efficiency of fifteen airtight membranes to reduce radon levels, also in combination with room pressurization. The results of these experiments were considered together with previous ones to propose the scale model room approach as a tool for rapidly evaluating the performance of specially designed radon barrier materials, and for radiation exposure assessment. Relative reduction of indoor radon (RIR) ranges from −20 to −94%. The most effective materials were FPO membrane, single-component silane-terminated polymer membranes and synthetic resins. The presence of additives likely modified the composition and structure of some products, improving their radon barrier capacity. The introduction of room pressurization further reduced radon levels in the model room where the membranes were applied. The overpressure necessary to reach RIRs of the order of 85–90% is very low for materials that powerfully stop radon even without ventilation, but necessarily higher for poorer membranes.

Keywords: indoor radon; radon barrier materials; home ventilation; radon mitigation; scale model room approach; radiation exposure



Citation: Portaro, M.; Rocchetti, I.; Tuccimei, P.; Galli, G.; Soligo, M.; Longoni, C.; Vasquez, D. The Scale Model Room Approach to Test the Performance of Airtight Membranes to Control Indoor Radon Levels and Radiation Exposure. *Atmosphere* **2024**, *15*, 1260. <https://doi.org/10.3390/atmos15101260>

Academic Editor: Chutima Kranrod

Received: 6 September 2024

Revised: 14 October 2024

Accepted: 18 October 2024

Published: 21 October 2024



Copyright: © 2024 by the authors. Licensee MDPI, Basel, Switzerland. This article is an open access article distributed under the terms and conditions of the Creative Commons Attribution (CC BY) license (<https://creativecommons.org/licenses/by/4.0/>).

1. Introduction

Indoor radon is one of the most significant contributors to lung cancer after smoking [1–3]. It can seep into indoor spaces through small cracks and openings in the foundations from soil enriched in its precursors or from building materials when the house is built with products with high radon emission [4,5].

Active and passive techniques are usually employed to reduce indoor radon concentration either as a preventive measure or as a corrective action [6–9]. Among them, the use of waterproof membranes in the crawl space of a building, or on the walls of edifices constructed with high radon-emitting materials, is widespread [10–13]. Ref. [14] proposed the use of single and double layers of wallpaper, also coupled to an intermediate layer of aluminum film, to mitigate radon exhalation from building materials.

The performance of airtight products as radon barriers is generally assessed using the radon diffusion coefficient (D , $\text{m}^2 \text{s}^{-1}$) of the waterproof material according to standard protocols [15–17]. Materials with D values in the order of 10^{-11} – $10^{-12} \text{ m}^2 \text{ s}^{-1}$ are the

most widespread and are considered suitable as radon barriers. Despite the publication of a reference method from the International Standardization Organization (ISO) [18], the measurement of radon diffusion coefficient still presents problems [16].

Recently, Ref. [19] proposed an alternative and complementary approach to test airtight products based on the relative change of indoor radon (RIR) in a scale model room after applying the material to be tested on its internal walls. The model room is a scaled version of the reference room defined by the European Commission [20] and is also very useful for quickly testing new materials when specially modified during the development phase by manufacturing companies. The system also has the aim of evaluating how the combined effect of forced ventilation at different rates in the chamber can (or cannot) modify radon levels.

The experimental configuration and procedures are perfectly reproducible, allowing standardized comparisons among products. The first thirteen products including the plasterboard support were tested in [19]. An evaluation of fifteen other materials chosen from the most used ones on the market and a general discussion are provided here. The membranes were also selected with the idea of guaranteeing easy implementation of the radon gas barrier system.

Finally, the model room approach is compared with the standard application of radon diffusion coefficients and is proposed as a routine tool for screening airtight products. The implications of this methodology for radiation exposure assessment are also addressed.

2. Materials and Methods

This section describes radon barrier materials and the model room approach used to characterize their performance.

2.1. Radon Barrier Materials

Fifteen commercial membranes widely available on the market were tested as barriers to radon. Their general composition is known, but detailed information on specific additives or quantitative ratios between components is secret for confidentiality reasons. They were polyurethanic membranes, mineral slurries, cement-based mortars, high-density polyethylene (HDPE) products, silane-terminated polymer membranes, a silicone sealant, epoxy and synthetic resins.

The samples were first glued or spread on 11 mm-thick plasterboard panels according to current operative procedures in the construction sector (see Table 1 for details) and then fixed with silicone on the walls of the room.

2.2. Experimental Configuration

The experimental configuration and procedures are well and thoroughly described in [19]. To avoid overlaps and repetitions with that paper already published on atmosphere, the methodology is briefly illustrated in this work in its most important parts. The system consists of the scale model room, two types of radon meters, a couple of flowmeters and vinyl tubing (Figure 1).

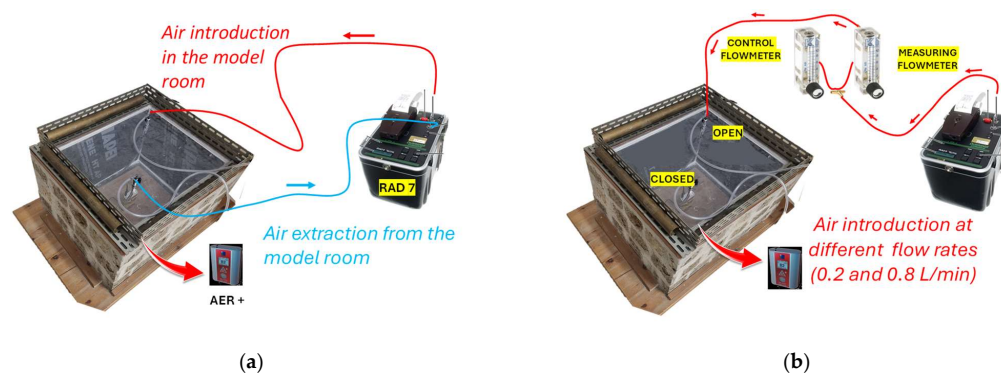


Figure 1. Experimental configuration during phases 1 and 2 (a) and for phases 3 and 4 (b). See Section 2.3 for details.

Table 1. Equilibrium ^{222}Rn and RIR values (% in parentheses) achieved in the scale model room in the different experimental phases. See Section 2.3 for details.

Sample *	Product	Application kg m^{-2}	Equilibrium ^{222}Rn Bq m^{-3}			
			Part 1	Part 2	Part 3	Part 4
A1	Plasterboard panel	-	1203 ± 121	1217 ± 93 (1)	808 ± 144 (−33)	436 ± 89 (−64)
A2	Mapethene HT AP	-	1217 ± 80	765 ± 78 (−37)	279 ± 79 (−77)	120 ± 49 (−90)
A3	Plastimul 2K Plus	4.3	1301 ± 196	830 ± 78 (−36)	311 ± 83 (−76)	122 ± 60 (−91)
A4	Mapeproof SA	-	1415 ± 119	674 ± 63 (−52)	271 ± 92 (−81)	150 ± 64 (−89)
A5	Mapeproof AL 1200 AP	-	1498 ± 113	573 ± 105 (−62)	275 ± 54 (−82)	116 ± 37 (−92)
A6	Plastimul 1K Superplus	2.3	1166 ± 213	687 ± 122 (−41)	301 ± 73 (−74)	106 ± 48 (−91)
A7	Mapelastac Aqua Defense	1	1842 ± 300	392 ± 67 (−79)	308 ± 110 (−83)	120 ± 57 (−93)
A8	Mapegum EPX-1	3	1464 ± 155	273 ± 51 (−81)	273 ± 105 (−81)	110 ± 58 (−93)
A9	Purtop 1000	2.2	1443 ± 169	841 ± 103 (−42)	220 ± 83 (−85)	145 ± 77 (−90)
A10	Purtop 611	2.2	1585 ± 191	1165 ± 133 (−27)	242 ± 76 (−85)	92 ± 41 (−94)
A11	Purtop 200	2.5	1428 ± 197	1170 ± 137 (−18)	322 ± 105 (−77)	129 ± 69 (−91)
A12	Purtop Easy DW	2.5	2041 ± 173	1273 ± 105 (−38)	362 ± 93 (−82)	129 ± 51 (−94)
A13	Aquaflex S1K	2.4	1920 ± 151	364 ± 63 (−81)	302 ± 90 (−84)	133 ± 63 (−93)
B1	Mapeproof Liquid Membrane	2.3	1378 ± 180	858 ± 106 (−38)	301 ± 88 (−78)	107 ± 44 (−92)
B2	Primer SN Rasante	1.4	1264 ± 162	666 ± 75 (−47)	126 ± 55 (−90)	90 ± 47 (−93)
B3	Sopro ZR Turbo MAXX 618	-	1449 ± 167	662 ± 56 (−54)	176 ± 66 (−88)	86 ± 34 (−94)
B4	Mapefloor I302 SL	2 + 1 Q 0.25	1324 ± 163	463 ± 60 (−65)	117 ± 51 (−91)	89 ± 52 (−93)
B5	Ultratop	34	1476 ± 114	1188 ± 116 (−20)	413 ± 96 (−72)	158 ± 62 (−89)
B6	Mapeproof AL AP	-	1336 ± 168	104 ± 31 (−92)	150 ± 51 (−89)	41 ± 23 (−97)
B7	Mapeproof FBT	-	1226 ± 73	125 ± 26 (−90)	136 ± 58 (−89)	81 ± 31 (−93)
B8	Planiseal CR1	2.2	1194 ± 99	293 ± 38 (−75)	89 ± 44 (−93)	73 ± 32 (−94)
B9	Purtop Easy	2.2	1266 ± 85	501 ± 41 (−60)	138 ± 56 (−89)	106 ± 43 (−92)
B10	Mapefloor PU 406	2.2	1239 ± 105	70 ± 24 (−94)	78 ± 33 (−94)	68 ± 31 (−94)
B11	Mapegum WPS	1.2	1601 ± 110	161 ± 39 (−90)	200 ± 75 (−87)	95 ± 46 (−94)
B12	Aquaflex Roof HR	2	1539 ± 225	217 ± 43 (−86)	212 ± 72 (−86)	113 ± 59 (−93)
B13	Mapefloor PU 406, no zeolites	-	1446 ± 122	666 ± 120 (−54)	177 ± 65 (−88)	235 ± 130 (−84)
B14	Sililate membrane, polymer only	-	1955 ± 122	671 ± 122 (−66)	382 ± 156 (−80)	212 ± 130 (−89)
B15	Mapesil BM	5	1423 ± 172	148 ± 31 (−90)	196 ± 76 (−86)	127 ± 49 (−91)

* The letter B is placed in front of the sample number to distinguish samples analyzed in this work from those tested in [19], identified with the letter A. As regards the latter, sample A2 is a bitumen membrane; samples A3 and A6 are bitumen emulsions; samples A4 and A5 are HDPE membranes; samples A7 and A8 are synthetic resins; samples A9, A10 and A11 are polyurea-based membranes; sample A12 is a polyurethane membrane; sample A13 is a silane terminated polymer. With reference to the new samples, samples B1, B10 and B13 are two-component polyurethane membranes; sample B9 is a single-component polyurethane membrane; samples B2 and B4 are two-component epoxy products; sample B3 is mineral slurry; sample B5 is a cement-based mortar; sample B6 is an HDPE membrane; sample B7 is an FPO membrane; samples B8 and B14 are silane-terminated polymers; samples B11 and B12 are synthetic resins; sample B15 is a silicone sealant. All radon data have been reported to a reference temperature of 23 °C. Errors are quoted as one standard deviation. The numbers in brackets are the relative changes in indoor radon (RIR) detected in the second, third or fourth part of each experiment with respect to the reference radon level in the first part.

The scale model room [19,21,22] is a 62 cm × 50 cm × 35 cm (length × width × height) chamber made of a high radon-emitting ignimbrite from Vico Volcano (Lazio, central Italy). Only the walls of the room were built with the stone, while the roof and the floor were made of Plexiglas panels. Two taps located on the upper Plexiglas panel allow air introduction and extraction and the connection to a RAD7 (DurrIDGE Company Inc., Billerica, MA, USA) radon monitor.

Another device, the AER PLUS (Algae Instrumentation, Bessines-sur-Gartempe, France), is placed in the model room for radon detection. Finally, two flowmeters (one measuring and the other controlling) are inserted in the circuit between the RAD7 outlet and the model room input tap to regulate the air flow. Further information on RAD7 and AER PLUS monitors is provided in Appendix A.

2.3. Experiments

Experiments were divided into four parts. At the beginning of the test, the walls of the model room were not covered with any material (part 1); an airtight product was then applied on its internal walls (part 2), and finally outdoor air was introduced in the chamber with a flow of 0.2 L min^{−1} (part 3) and 0.8 L min^{−1} (part 4). In order to make the results

of the experiments more exportable, the air flow rates (AFR, $L \text{ min}^{-1}$) were expressed as air exchange rates (ACH, h^{-1}) by dividing the AFR by the volume of the model room ($V = 0.110 \text{ m}^3$) and multiplying by 60.

$$\text{ACH} = \text{AFR}/V \quad (1)$$

The ACH values for parts 3 and 4 were found to be 0.11 h^{-1} and 0.44 h^{-1} , respectively. The RAD7 and AER PLUS monitors were used in the first and second parts of the experiments, while only the AER PLUS was employed in the third and fourth parts, with the RAD7 used to pump air in the model room. A measurement interval of 1 h was selected for both instruments.

The indoor radon obtained from the four phases corresponded to equilibrium radon activity concentrations, generally calculated by averaging activity concentration from the 25th hour of each measurement phase up to the end of them (lasting at least 48 h). The standard deviation from the mean of different experimental parts was used to demonstrate that the equilibrium of radon activity concentration was generally reached after 24 h within the error range (see Appendix C in [19]).

Equilibrium radon data (R_n) were reported to a reference temperature of $23 \text{ }^\circ\text{C}$ (R_{n23}) to consider the effect of temperature on radon exhalation according to Equation (2) [19].

$$R_{n23} = R_n \times 23/T_{\text{ambient}} \quad (2)$$

The relative change of indoor radon (RIR) for parts 2, 3 and 4 was found by applying Equation (3).

$$\text{RIR} = (R_{nB} - R_{nA})/R_{nA} \times 100 \quad (3)$$

where R_{nA} is the equilibrium radon activity from part 1 and R_{nB} are equilibrium radon data from parts 2, 3 and 4, all reported at $23 \text{ }^\circ\text{C}$.

3. Results

Experimental results are reported in Table 1, together with those analyzed in [19], to give a complete view of the data. Equilibrium radon activity concentrations, normalized at $23 \text{ }^\circ\text{C}$, are quoted as the average plus or minus one standard deviation from the mean, as stated in Section 2.3. The standard deviations calculated for high radon levels or measured with the RAD7 are relatively lower than those for low radon activity concentrations or obtained with the AER PLUS.

Relative humidity in the course of the experiments ranged from 45 to 59%. A specific correction for the effect of humidity on radon exhalation from the walls of the chamber was not applied because the laboratory conditions were quite constant, affecting the exhalation no more than 10% [23].

The average equilibrium radon in the model room related to the first part of the experiments (no panels on the walls) was $1370 \pm 125 \text{ Bq m}^{-3}$ (this work).

RIR values in the second part of the experiments (with panels on the walls) range from -20% (sample B5, a cement-based mortar) to -94% (sample B10, a two-component polyurethane binder with zeolites). Looking more closely at Table 1, it is possible to group the samples into four classes (Table 2), based on RIR values only (see the next section for further details): class 1 (samples with low RIR, $\leq 44\%$), class 2 (samples with intermediate RIR ranging from -45% to -65%), class 3 (samples with high RIR, always better than -66%) and class 4 (samples with a wide range of RIR between -38% and -94%). Sample B5 is the only component of group 1, while samples B2, B3 and B4 belong to group 2; samples B7, B8, B11, B12, B14 and B15 fall into group 3, and samples B1, B6, B9, B10 and B13 can be assigned to group 4. An in-depth discussion of these findings, also extended to materials analyzed in [19], is presented in Section 4 (Table 2).

Table 2. Airtight membranes tested with the model room approach grouped into four classes based on the relative change of indoor radon (RIR, %) in the second phase of the experiments.

Class *	Type	Number of Samples	Samples **	RIR (% , Phase II of the Experiments)
1	Cement-based mortar	1	B5	−20
	Self-adhesive bituminous membrane	1	A2	−37
	Bituminous emulsions	2	A3, A6	from −36 to −41
	Polyurea-based membranes	3	A9, A10, A11	from −18 to −42
2	Epoxy compounds	2	B2, B4	from −47 to −65
	Mineral slurry	1	B3	−54
3	FPO membrane	1	B7	−90
	Silane-terminated polymer membranes	3	B8, B14, A13	from −66 to −81
	Synthetic resin	4	B11, B12, A7, A8	from −79 to −90
	Silicon sealant	1	B15	−90
4	Polyurethanes	5	B1, B9, B10, B13, A12	from −38 to −94
	HDPE membranes	3	B6, A4, A5	from −52 to −92

* Classes 1, 2, 3 and 4 refer to samples with RIR $\leq -44\%$, between -45% and -65% , $\geq 66\%$ and from -38% to -94% , respectively. ** Samples reported in [19] are labelled with the letter A before the sample number (see Table 2 in [19]), while those tested in this work have the letter B in front of the sample number.

Finally, radon reduction in part 3 (with panels and ACH of 0.11 h^{-1}) varies between -72% (sample B5) and -94% (sample B10), while it ranges from -85% (sample B14, a silane-terminated polymer) to -97% (sample B6, a HDPE membrane) in part 4 (with panels and ACH of 0.44 h^{-1}).

4. Discussion

Table 2 reports the complete list of materials tested with the model room, either those analyzed in [19] or new data provided here. In the case of the materials studied in [19], the letter A is placed in front of the sample number (see also Appendix B, Table A1), while the samples tested in this work (Table 1) are labelled with the letter B before the numerical code.

According to the experimental results, airtight materials tested with the model room approach can be grouped into four classes based on their RIR only. The boundaries between adjacent classes were chosen to include the greatest number of samples with a comparable overall composition in the same group, leaving in a separate class those with a very distinct behavior despite the similar composition. The presence of additives is known only for the fourth class. Due to the lack of data on the specific nature of each sample (i.e., presence of additives, etc.), materials indicated with the same name could fall into different classes. This would make it very difficult to treat RIR values statistically, as any approach would be affected by this knowledge gap. In the following discussion, the RIR values obtained with the model room are compared with studies on radon diffusion coefficients, because to our knowledge there are no studies that use an approach like ours to test radon barrier materials.

Class 1 includes cement-based mortars, self-adhesive bituminous membrane, bituminous emulsions and polyurea-based membranes. These kinds of materials always provided $\text{RIR} \leq -44\%$. Sample B5, a cement-based mortar, showed a -20% reduction in radon, making it the worst product among those tested with the model room. The unsatisfactory behavior of cement and concrete has been widely documented in the literature by values of radon diffusion coefficients in the order of 10^{-7} – $10^{-8} \text{ m}^2 \text{ s}^{-1}$ [24–27]. A better performance was provided by bitumen-based products; samples A2, A3 and A6 gave RIRs of -37% , -36% and -41% , respectively. Bitumen-based membranes are commonly used in construction, and their fair performance is validated by D values in the order of $10^{-11} \text{ m}^2 \text{ s}^{-1}$, as also reported in [16,28,29]. A poor performance was offered by polyurea-based membranes, although a progressive improvement from -18% (sample A11) to -27% (sample A10) and -42% (sample A9) can be ascribed to a gradual decrease in porosity, in turn related to a higher concentration of hydrogen bonds and degree of branching in the structure

of polyurea-based polymers [19]. Literature on radon barrier properties of this kind of product is limited.

Class 2 contains products with intermediate performances (RIRs from -45% to -65%), epoxy compounds (B2 and B4) and a two-component modified mineral mortar (B3). Samples B2 and B4 gave RIR values of -47% and -65% , respectively, with sample B4 containing a high solids content, apparently improving its radon barrier properties. Epoxy materials are commonly used in construction [30] and rated as good products thanks to radon diffusion coefficients in the order of $10^{-12} \text{ m}^2 \text{ s}^{-1}$ [16,29]. Sample B3 provided a radon reduction of -54% . These kinds of materials are often employed as joint fillers or as floor levelers.

Class 3 includes the products with the best performances (RIR always greater than -66%): an FPO membrane (sample B7), one-component silane-terminated polymer membranes (samples B8, B14 and A13), synthetic resins (samples B11, B12, A7 and A8) and a silicone sealant (B15). Sample B7 gave a radon reduction of -90% ; samples B8 and B14 behaved similarly with RIR of -75% and -66% , respectively, slightly worse than sample A13 (RIR of -81%), demonstrating that, regardless of specific composition, silane-terminated polymers are excellent products. Product A13 was also used in a case-study to treat the internal walls of a single-family house in Celleno town (central Italy) made of a tuff very rich in radon precursors [13]. After its application, indoor radon was reduced from 2776 Bq m^{-3} to 1475 Bq m^{-3} . The further ventilation of a cavity behind the walls of a semi-buried room brought the radon level down to a few hundreds Bq m^{-3} . As far as synthetic resins are concerned, their radon reductions were outstanding: sample B11 (RIR = -90%), sample B12 (RIR = -86%), sample A8 (RIR = -81%) and sample A7 (RIR = -79%). These types of products are widely used to insulate buildings against radon entry. Finally, sample B15 provided a radon reduction of -90% , showing excellent ability to prevent radon diffusion and to seal junction boxes and pass-through bodies.

Class 4 contains materials with a large range of RIR values, mainly polyurethanes and HDPE membranes. These materials behaved differently depending on the additives used. Starting from polyurethanes, sample B1, a two-component polyurethane, gave an RIR of -38% , as did sample A12, characterized by a similar composition. Sample B9, a one-component polyurethane, performed better (RIR = -60%), with results comparable with those of another two-component polyurethane (sample B13), with RIR of -54% . The addition of zeolites brought the RIR values of the product from -54% (sample B13) to -94% (sample B10), showing that a membrane with a good performance [17] may become excellent if solids capable of absorbing radon in their structure are employed. These minerals are routinely used to capture and store CO_2 [31] and separate it from other gases such as CH_4 or N_2 because of their microporous structure. The ability of zeolites to adsorb radon is well-described by [32]; Ref. [33] reported on the use of silver-exchanged zeolites to adsorb radon; Ref. [34] investigated the potential of natural zeolites to achieve this goal, while [35] studied the radon adsorption of artificial zeolites combined with blue silica gel.

From what has been reported so far, it is evident that the composition and porosity of polymers influence their radon barrier properties, but this works for single-component membranes, as in the case of polyurea-based membranes (A9, A10 and A11). However, the use of additives may change the structure of the product or modify its radon adsorption (samples B10 and B13), significantly changing its performance.

Another observation concerns the behavior of these materials, which could change due to their aging. For example, [26] found that radon diffusion coefficients of 17- to 45-year-old cements in Florida increased by 1.6. A similar result was reported by [36], which observed changes in D values up to 83% for bitumen and polymers exposed to degradation agents such as radon, soil bacteria and high temperatures. Finally, [37] suggests that radon levels should be measured at periodic intervals after remediation, perhaps once every 5 years, to ensure that concentrations continue to remain at acceptable levels.

The discussion developed so far was focused on the experimental results obtained without considering the effect of air exchange (parts 1 and 2 of the experiments). The introduction of air into the model room with exchange rates of 0.11 h^{-1} (part 3) and

0.44 h^{-1} (part 4) clearly shows that room pressurization improved the radon reduction of all samples and that the higher the air exchange, the stronger the indoor radon drop (Figure 2).

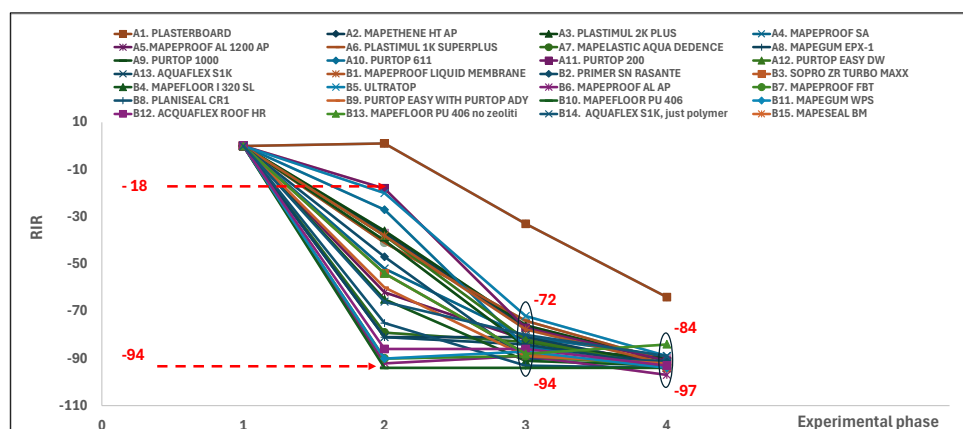


Figure 2. Relative change of indoor radon (RIR) during the four parts of 28 experiments. See text, Table 1 (this work) and Figure 3 and Table 2 [19] for explanation.

This is demonstrated by the range of RIR values obtained in experimental parts 2, 3 and 4: from -18% (sample A11) to -94% (sample B10) in part 2; from -80% (sample B14) to -94% (sample B10) in part 3; from -84% (sample B13) to -97% (samples B6) in part 4. As a result, the differences between the materials are reduced after activating the room pressurization, and products with better performance require a lower overpressure to achieve radon reduction of the order of 85–90%, with evident energy and cost savings. This allows experts to design the air exchange system suited to specific conditions, choose a suitable motor and establish the operation and shutdown times of ventilation devices.

The model room approach represents an excellent and direct tool for validating the performance of radon barrier materials because it is based on a simple principle, namely on the relative reduction in indoor radon (RIR), with reference to an initial condition in which the membrane is not applied in the internal walls of the chamber. The model room is a scale version of a model chamber originally proposed by EC 1999 [20], to control and protect against natural radiation exposure due to building material. Our approach exploits building materials as a source of radon, but indoor radon reduction can be applied to indoor radon regardless of its source [19,21,22]. This methodology is useful for guiding manufacturing companies in the production of new membranes and in the choice of specific additives that have proven promising in retaining radon.

Furthermore, it is possible to implement the dataset by introducing the forced ventilation effect. On this basis, we propose the scale model room approach as an alternative or in combination with standard methods based on the determination of radon diffusion coefficients of insulating materials according to [18]. This standard specifies the assumptions and boundary conditions that should be met, but despite this, several laboratories still provide discrepant results due to inadequate experimental setup and calculation methods [38,39].

We also intend to support the model room approach for the evaluation of radiation exposure due to radon in closed environments. Since the effective dose due to radon exposure is directly proportional to indoor radon level [40], the RIR data could be easily transformed into a percentage reduction in the effective dose. This implication makes the model room approach for the validation of waterproof membranes particularly advantageous compared to other methods based on radon diffusion coefficients, strengthening its additional use in the context of radiation exposure.

5. Conclusions

The main conclusions of this study can be summarized as follows:

- The scale model room approach is a very useful tool to test the performance of waterproof materials. It is a rapid and straightforward method to evaluate the indoor radon reduction in consistent settings and compare different membranes, even during the production and development stages.
- This methodology is useful for guiding manufacturing companies in the production of new membranes and in the choice of specific additives that have proven promising in retaining radon in this screening phase.
- The model room is here proposed as an alternative or in combination with the standard approach based on radon diffusion coefficients which still presents difficulties in measurement by different laboratories.
- It is not intended to reproduce real conditions and situations or evaluate the scale ratios between radon levels and size/volume of the indoor environment, but it is useful for practical applications because it provides indications of best materials.
- This approach is also helpful for evaluating the relative reduction in radiation exposure, i.e., the exposure directly proportional to indoor radon activity concentrations.

Author Contributions: M.P., I.R., P.T., M.S. and G.G. were equally involved in conceptualization, methodology, formal analysis, investigation and writing. C.L. and D.V. participated in investigation and validation. All authors have read and agreed to the published version of the manuscript.

Funding: This research was carried out in the frame of a PhD project, funded by Università degli Studi “Roma Tre”, PON DM 1061. The project also benefitted from funding from Dipartimento di Scienze, Università “Roma Tre” (MIUR—Italy, Dipartimento di Eccellenza, Articolo 1, Commi 314–337 Legge 232/2016). C.L. and D.V. provided us with the products to be tested.

Institutional Review Board Statement: Not applicable.

Informed Consent Statement: Not applicable.

Data Availability Statement: All data are reported in the present manuscript and in [19].

Acknowledgments: Authors wish to thank Carlo Lucchetti and Mauro Castelluccio, who designed and built the model room within the EU-funded LIFE-RESPIRE project, performing the first measurements [21]. Antonio Ausilio and Marco De Ciechi (MAPEI S.p.A.) are acknowledged for the selection of materials to be tested and for the useful suggestions on data interpretation.

Conflicts of Interest: Authors Cristina Longoni and Dino Vasquez were employed by the company Mapei S.p.A. The remaining authors declare that the research was conducted in the absence of any commercial or financial relationships that could be construed as a potential conflict of interest.

Appendix A

The RAD7 is a continuous radon monitor that collects radon and thoron daughters (polonium isotopes) on the surface of its planar silicon detector, enabling high-resolution alpha spectroscopy of their decay energies. The instrument is equipped with a built-in pump to exchange air with the environment or with vials or chambers connected to it in a closed air loop. Temperature and relative humidity data are collected throughout the run. The AER PLUS is a small solid-state radon detector with local storage for temperature and relative humidity data. It is battery-supplied with an autonomy of one year.

The effect of water molecules on the electrostatic collection of ^{218}Po ions (^{222}Rn daughters) onto the surface of the AER PLUS and RAD7 silicon detectors (neutralization) was evaluated through comparison with the Istituto Nazionale di Geofisica e Vulcanologia (INGV, Roma, Italy) radon chamber equipped with a scintillation cell (ZnS), which is not affected by air humidity. Absolute humidity (AH) reduces the efficiency of radon detectors and needs to be accounted for. Specific corrections for the RAD7 and AER PLUS as a function of AH are reported in [19].

Appendix B

A complete list of relative change in indoor radon (RIR) data obtained in parts 2, 3 and 4 of the experiments is given in Table A1. It includes samples considered in [19] and materials analyzed in this work.

Table A1. Relative change of indoor radon (RIR, %) of airtight products (those reported in [19] and in this work) using the model room approach.

Sample *	Relative Indoor Radon Change		
	Part 2	Part 3	Part 4
A1	1	−33	−64
A2	−37	−77	−90
A3	−36	−76	−91
A4	−52	−81	−89
A5	−62	−82	−92
A6	−41	−74	−91
A7	−79	−83	−93
A8	−81	−81	−93
A9	−42	−85	−90
A10	−27	−85	−94
A11	−18	−77	−91
A12	−38	−82	−94
A13	−81	−84	−93
B1	−38	−78	−92
B2	−47	−90	−93
B3	−54	−88	−94
B4	−65	−91	−93
B5	−20	−72	−89
B6	−92	−89	−97
B7	−90	−89	−93
B8	−75	−93	−94
B9	−60	−89	−92
B10	−94	−94	−94
B11	−90	−87	−94
B12	−86	−86	−93
B13	−54	−88	−84
B14	−66	−80	−89
B15	−90	−86	−91

* In the case of the materials studied in [19], the letter A is placed in front of the sample number. The samples tested in this work (Table 1) are labelled with the letter B before the numerical code.

References

- Sethi, T.K.; El-Ghamry, M.N.; Kloecker, G.H. Radon and Lung Cancer. *Clin. Adv. Hematol. Oncol.* **2012**, *10*, 157–164. [[PubMed](#)]
- Riudavets, M.; Garcia de Herreros, M.; Besse, B.; Mezquit, L. Radon and Lung Cancer. *Curr. Trends Future Perspect. Cancers* **2022**, *14*, 3142.
- Schabath, M.B.; Cote, M.L. Cancer Progress and Priorities: Lung Cancer. *Cancer Epidemiol. Biomark. Prev.* **2019**, *10*, 1563–1579. [[CrossRef](#)] [[PubMed](#)]
- Bruno, R.C. Sources of Indoor Radon in Houses: A Review. *J. Air Pollut. Control Assoc.* **1983**, *33*, 105–109. [[CrossRef](#)]
- Vogiannis, E.G.; Nikolopoulos, D. Radon sources and associated risk in terms of exposure and dose. *Front. Public Health* **2014**, *2*, 207. [[CrossRef](#)]
- Henschel, D.B. Analysis of Radon Mitigation Techniques Used in Existing US Houses. *Radiat. Prot. Dosim.* **1994**, *56*, 21–27.
- Steck, D.J. The Effectiveness of Mitigation for Reducing Radon Risk in Single-Family Minnesota Homes. *Health Phys.* **2012**, *103*, 241–248. [[CrossRef](#)]
- Fuente, M.; Rabágo, D.; Goggins, J.; Fuente, I.; Sainz, C.; Foley, M. Radon concentration and pressure field extension monitoring in a pilot house in Spain. *Sci. Total Environ.* **2019**, *695*, 133746. [[CrossRef](#)]
- Khan, S.M.; Gomes, J.; Krewski, D.R. Radon interventions around the globe: A systematic review. *Heliyon* **2019**, *5*, e011737. [[CrossRef](#)]
- Baltrocchi, A.P.D.; Maggi, L.; Dal Lago, B.; Torretta, V.; Szabó, M.; Nasirov, M.; Kabilov, E.; Rada, E.C. Mechanisms of Diffusion of Radon in Buildings and Mitigation Techniques. *Sustainability* **2024**, *16*, 324. [[CrossRef](#)]

11. Mortazavi, S.M.J.; Jamali, F.; Moradgholi, J.; Mehdizadeh, A.R.; Faghihi, R.; Mehdizadeh, F.; Haghani, M.; Saieedi, M.; Mortazavi, S.A.; Ghanbarpour, M.R. Investigation of the Efficacy of Damp-Proof Montmorillonite Nanoclay for Radon Reduction Strategies in Radon Prone Areas of Ramsar. *J. Biomed. Phys. Eng.* **2013**, *3*, 25–28.
12. Jiránek, M.; Hůlka, J. Applicability of various insulating materials for radon barriers. *Sci. Total Environ.* **2001**, *272*, 79–84. [[CrossRef](#)] [[PubMed](#)]
13. Portaro, M.; Rocchetti, I.; Tuccimei, P.; Galli, G.; Soligo, M.; Ciotoli, G.; Longoni, C.; Vasquez, D.; Sola, F. Indoor Radon Surveying and Mitigation in the Case-Study of Celleno Town (Central Italy) Located in a Medium Geogenic Radon Potential Area. *Atmosphere* **2024**, *15*, 425. [[CrossRef](#)]
14. Ruvira, B.; García-Fayos, B.; García-Gimeno, B.; Arnal, J.M.; Verdú, G. Study of the use of wallpaper to mitigate radon exhalation from building materials in indoor spaces. *Radiat. Phys. Chem.* **2024**, *223*, 111916. [[CrossRef](#)]
15. Jiránek, M.; Hůlka, J. Radon diffusion coefficient in radon-proof membranes—Determination and applicability for the design of radon barriers. *Int. J. Archit. Sci.* **2000**, *1*, 149–155.
16. Jiránek, M.; Kotrbatá, M. Radon diffusion coefficients in 360 waterproof materials of different chemical composition. *Radiat. Prot. Dosim.* **2011**, *145*, 178–183. [[CrossRef](#)]
17. Tejado-Ramos, J.-J.; Alvarez-Toral, A.; Guillén, J.; Carmona, M.; Muñoz-Almaraz, F.J. Methodology for assessment of radon diffusion coefficients in membranes, used as radon barriers in construction and refurbishment. *Constr. Build. Mater.* **2024**, *414*, 134967. [[CrossRef](#)]
18. ISO/TS 11665–13; Measurement of Radioactivity in the Environment—Air: Radon 222—Part 13: Determination of the Diffusion Coefficient in Waterproof Materials: Membrane Two-Side Activity Concentration Test Method. International Standardization Organization (ISO): Geneva, Switzerland, 2017.
19. Portaro, M.; Tuccimei, P.; Galli, G.; Soligo, M.; Longoni, C.; Vasquez, D. Testing the properties of radon barrier materials and home ventilation to reduce indoor radon accumulation. *Atmosphere* **2023**, *14*, 15. [[CrossRef](#)]
20. EC (European Council). Directorate-General for Environment. Radiological protection principles concerning the natural radioactivity of building material. *Radiat. Prot.* **1999**, *112*, 1–16.
21. Lucchetti, C.; Castelluccio, M.; Altamore, M.; Briganti, A.; Galli, G.; Soligo, M.; Tuccimei, P.; Voltaggio, M. Using a scale model room to assess the contribution of building material of volcanic origin to indoor radon. *Nukleonika* **2020**, *65*, 71–76. [[CrossRef](#)]
22. Lucchetti, C.; Galli, G.; Tuccimei, P. Indoor/outdoor air exchange affects indoor radon. The use of a scale model room to develop a mitigation strategy. *Adv. Geosci.* **2022**, *57*, 81–88. [[CrossRef](#)]
23. Tuccimei, P.; Moroni, M.; Norcia, D. Simultaneous determination of ²²²Rn and ²²⁰Rn exhalation rates from building materials used in Central Italy with accumulation chambers and a continuous solid state alpha detector: Influence of particle size, humidity and precursors concentration. *Appl. Radiat. Isot.* **2006**, *64*, 254–263. [[CrossRef](#)] [[PubMed](#)]
24. Gadd, M.S.; Borak, T.B. In-situ determination of the diffusion coefficient of ²²²Rn in concrete. *Health Phys.* **1995**, *68*, 817–822. [[CrossRef](#)] [[PubMed](#)]
25. Rogers, V.C.; Nielson, K.K.; Holt, R.B.; Snoddy, R. Radon diffusion coefficients for residential concretes. *Health Phys.* **1994**, *67*, 261–265. [[CrossRef](#)]
26. Rogers, V.C.; Nielson, K.K. *Economic Impact Statement for Radon Control Features in New Residential Construction*; report RAE-9226/2-5; Rogers & Associates Engineering Corp.: Salt Lake City, UT, USA, 1994.
27. Chauhan, R.P.; Kumar, A. A Comparative Study of Indoor Radon Contributed by Diffusive and Advective Transport through Intact Concrete. *Phys. Procedia* **2015**, *80*, 109–112. [[CrossRef](#)]
28. Gaskin, J.; Li, Y.E.; Ganapathy, G.; Nong, G.; Whyte, J.; Zhou, L.G. Radon infiltration building envelope test system: Evaluation of barrier Materials. *Radiat. Prot. Dosim.* **2021**, *196*, 17–25. [[CrossRef](#)]
29. Sainz, C.; Gutiérrez, J.L.; Quindós, L.S.; Fuente, I. Radon Diffusion Coefficient in FOAMGLAS® Cellular Glass Thermal Insulation. Report RAD592_E2. 2016. Available online: <https://www.foamglas.com> (accessed on 4 July 2024).
30. Rasmussen, T.V.; Cornelius, T. Use of radon barriers to reach an acceptable radon level. *E3S Web Conf.* **2020**, *172*, 05003. [[CrossRef](#)]
31. Boer, D.G.; Langerak, J.; Pescarmona, P.P. Zeolites as Selective Adsorbents for CO₂ Separation. *ACS Appl. Energy Mater.* **2023**, *6*, 2634–2656. [[CrossRef](#)]
32. Bikit, I.; Mrdja, D.; Bikit, K.; Grujic, S.; Knezevic, D.; Forkapic, S.; Kozmidis-Luburic, U. Radon adsorption by zeolite. *Radiat. Meas.* **2015**, *72*, 70–74. [[CrossRef](#)]
33. Heinitz, S.; Mermans, J.; Maertens, D.; Skliarova, H.; Aerts, A.; Cardinaels, T.; Gueibe, C.; Rutten, J.; Ireland, N.; Kuznicki, D.; et al. Adsorption of radon on silver exchanged zeolites at ambient temperatures. *Sci. Rep.* **2023**, *13*, 6811. [[CrossRef](#)]
34. Gagliardo, G.; Hanfi, M.Y.; La Verde, G.; Pugliese, M.; Gargiulo, N.; Caputo, D.; Ambrosino, F. Efficacy of zeolites in radon adsorption: State of the art and development of an optimized approach. *Isot. Environ. Health Stud.* **2024**, *60*, 471–484. [[CrossRef](#)] [[PubMed](#)]
35. Paschalides, J.S.; Marinakis, G.S.; Petropoulos, N. Passive, integrated measurement of radon using 5A synthetic zeolite and blue silica gel. *Appl. Radiat. Isot.* **2009**, *68*, 15–16. [[CrossRef](#)] [[PubMed](#)]
36. Rovenská, K.N. The effect on the radon diffusion coefficient of long-term exposure of waterproof membranes to various degradation agents. *Radiat. Prot. Dosim.* **2014**, *160*, 92–95. [[CrossRef](#)]
37. Rahman, N.M.; Tracy, B.L. Radon control systems in existing and new construction: A review. *Radiat. Prot. Dosim.* **2009**, *135*, 243–255. [[CrossRef](#)]

38. Rovenska, K.; Jiranek, M. 1st International comparison measurement on assessing the diffusion coefficient of radon. *Radiat. Prot. Dosim.* **2011**, *145*, 127–132. [[CrossRef](#)]
39. Rovenska, K.; Jiranek, M. Radon diffusion coefficient measurement in waterproofings—A review of methods and an analysis of differences in results. *Appl. Radiat. Isot.* **2012**, *70*, 802–807. [[CrossRef](#)]
40. Marsh, J.W.; Tomášek, L.; Laurier, D.; Harrison, J.D. Effective dose coefficients for radon and progeny: A review of ICRP and UNSCEAR values. *Radiat. Prot. Dosim.* **2021**, *195*, 1–20. [[CrossRef](#)]

Disclaimer/Publisher’s Note: The statements, opinions and data contained in all publications are solely those of the individual author(s) and contributor(s) and not of MDPI and/or the editor(s). MDPI and/or the editor(s) disclaim responsibility for any injury to people or property resulting from any ideas, methods, instructions or products referred to in the content.